

APPLICATIONS OF A DPCM SYSTEM WITH MEDIAN PREDICTORS FOR IMAGE CODING

Dong Hee Kang*, Jin Ho Choi*, Yong Hoon Lee* and Choon Lee**

*Department of Electrical Engineering
Korea Advanced Institute of Science and Technology
373-1 Kusong-Dong, Yusung-Gu, Taejeon, Korea 305-701
**Consumer Electronics Research Lab., GoldStar,
16, Woomyeon-Dong, Seocho-Gu, Seoul, Korea 137-140

ABSTRACT

A DPCM system employing a median predictor, which is called the predictive median-DPCM (PM-DPCM), is proposed. An interesting property that in PM-DPCM transmission noise is often isolated and not propagated over the reconstructed signals is observed and is analyzed deterministically and statistically.

In order to examine the performance characteristics of the PM-DPCM, it is applied to real image signals. The experimental results indicate that the PM-DPCM outperforms the standard DPCM when transmission errors occur, and that the former performs like the latter under noise-free conditions.

1. INTRODUCTION

Differential pulse code modulation (DPCM) is an efficient data compression technique, which is useful for reducing transmission rate of digital picture information. The use of DPCM in image coding, however, requires some caution when transmission errors occur, because in the reconstructed DPCM image transmission errors tend to propagate and severely degrade the image quality [1]. To overcome the difficulty, error robust schemes such as hybrid DPCM [1-3] have been proposed.

In this paper, we introduce a DPCM system employing nonlinear median predictors, which is called the predictive median (PM)-DPCM, and show that the PM-DPCM is resistant to transmission errors. Specifically, it is observed that transmission errors are often isolated and not propagated in the PM-DPCM images. We shall analyze the characteristics of PM-DPCM, and compare its performance with those of other DPCM systems through experiments.

The organization of this paper is as follows. In section 2, 1-D and 2-D PM-DPCM systems are defined and their properties are examined. In section 3, some statistical properties of PM-DPCM are derived. Experimental results are presented in section 4.

2. PREDICTIVE MEDIAN - DPCM

2.1 One-Dimensional PM-DPCM

Fig. 1 illustrates a DPCM system. In 1-D PM-DPCM the prediction $\hat{y}(n)$ of the input $y(n)$ is given by

$$\hat{y}(n) = \text{median}\{y(n-1), y(n-2), \dots, y(n-M)\} \quad (1)$$

where M is an odd integer. The PM-DPCM system is able to reconstruct an original signal at the receiver just like a DPCM system using a linear predictor. Neglecting the effect of quantizer [i.e., assuming the prediction error $x(n)$ is equal to the quantized prediction error $\hat{x}(n)$] and assuming noiseless transmission channel, the reconstructed signal $y_r(n)$ can be expressed as

$$y_r(n) = x(n) + \text{median}\{y_r(n-1), \dots, y_r(n-M)\} \quad (2)$$

If $y_r(n-i) = y(n-i)$, $i=1,2,\dots,M$ in Eq.(2), then $y_r(n) = y(n)$ because the prediction error signal $x(n)$ is

$$x(n) = y(n) - \text{median}\{y(n-1), \dots, y(n-M)\} \quad (3)$$

For example, consider Fig. 2 in which PM-DPCM with $M=3$ is applied to an input sequence (the initial values of $y(n)$ and $x(n)$ are set to zero). Note that the reconstructed signal $y_r(n)$ is identical to the original input signal $y(n)$.

The variance of prediction error of the PM-DPCM is usually larger than that of the standard DPCM with linear predictors. This fact is confirmed in the following section through statistical analysis. The robustness of the PM-DPCM to transmission errors can be seen from an example in Fig. 3. Fig. 3(a) and (b) depict the received prediction error signal $x_r(n)$ and the reconstructed signal $y_r(n)$, respectively, of the PM-DPCM which is considered in Fig. 2. (Again, for simplicity, quantization effects are neglected). The received signal $x_r(n)$ is identical to $x(n)$ in Fig. 2(c) except at $n=6$ where the signal value has been changed by a transmission error. It is interesting to note that reconstructed signal $y_r(n)$ is also identical to the signal in Fig. 2(d), which is reconstructed under noise-free conditions, except at $n=6$. The noisy value at $n=6$ has been isolated and not propagated over the reconstructed signals. This phenomenon is explained as follows. In Fig. 2(a) $y(6)$ is a local maximum value and cannot be the output of the median predictor at any time indices (see Fig. 2(b)). In Fig. 3(a), the transmission noise caused the reconstructed value $y_r(6)$ larger than the original value $y(6)$. Thus the predicted values of the decoder remain the same as those of the encoder, that is, for $n=7,8,9$

$$\text{median}\{y_r(n-1), y_r(n-2), y_r(n-3)\} = \text{median}\{y(n-1), y(n-2), y(n-3)\}, \quad (4)$$

and we get $y_r(n)=y(n)$. This example indicates that PM-DPCM can often isolate transmission bit errors. A sufficient condition for the error isolation is presented next.

Observation 1 : Assume only one error occurs at time index $n=n_0$, i.e., $x(n_0) \neq x_r(n_0)$ and $x(n) = x_r(n)$ for all $n \neq n_0$. The error is isolated if the reconstructed value $y_r(n_0)$ is greater (less) than $\text{median}\{y_r(n-1), y_r(n-2), \dots, y_r(n-M)\}$ whenever the original value $y(n_0)$ is greater (less) than $\text{median}\{y(n-1), y(n-2), \dots, y(n-M)\}$ for all n , $n_0 + 1 \leq n \leq n_0 + M$.

The proof of Observation 1 is obvious and thus omitted. For the case of multiple errors Observation 1 is not valid unless errors occur sparsely. Now we examine the case where an

error is not isolated but propagated. Assume again an error has occurred at time index n_0 . If we denote the propagation error by $e_p(n)$, $n > n_0$, then

$$\begin{aligned} e_p(n) &\equiv y_r(n) - y(n) \\ &= x_r(n) + \text{median}\{y_r(n-i), i=1, \dots, M\} \\ &\quad - [x(n) + \text{median}\{y(n-i), i=1, \dots, M\}] \\ &= \text{median}\{y_r(n-i), i=1, \dots, M\} - \\ &\quad \text{median}\{y(n-i), i=1, \dots, M\}, \end{aligned} \quad (5)$$

where the third equality holds because it is assumed that $x_r(n) = x(n)$ for $n > n_0$. For $n < n_0$, $e_p(n)$ is assumed to be zero. Next we show that $|e_p(n)|$ is smaller than the noise value at $n = n_0$. (Throughout the analysis, the effect of quantization is ignored.)

Observation 2: Suppose that a transmission error value e is superimposed on the signal $x(n)$ at time index n_0 , i.e., $x_r(n_0) = x(n_0) + e$. Then the propagation error $e_p(n)$ is bounded by

$$\begin{aligned} \min\{e_p(n-i), i=1, \dots, M\} \leq \\ e_p(n) \leq \max\{e_p(n-i), i=1, \dots, M\} \end{aligned} \quad (6)$$

for all $n > n_0$.

This observation shows that the present error $e_p(n)$ is bounded by the past errors $e_p(n-i)$, $i=1, \dots, M$. Since $0 \leq e_p(n_0+1) \leq |e|$ then $e_p(n_0) \leq |e|$ for all $n > n_0$.

Fig. 4 illustrates the performance characteristics of the proposed PM-DPCM ($M=3$) when it is applied to a row of an image. Fig. 4(a) and (b) show the input and the prediction error signal, respectively. The received prediction error signal in Fig. 4(c) has an error value $e=100$ at $n=150$. The reconstructed signal and the difference between the original signal and the reconstructed signal are shown in Fig. 4(d) and (e), respectively. In this case the transmission error has not been isolated, yet error propagation after $n=150$ is almost negligible. This is confirmed in Section 4 through experiments with real images.

Lastly in this subsection, it is pointed out that 1-D PM-DPCM loses edge information when a transmission error appears at edge locations of an input signal. This is illustrated by applying 1-D PM-DPCM to a binary input with an edge. Fig. 5(a) shows the performance of the PM-DPCM ($M=3$) under noise-free conditions. As expected, the original binary signal having an edge is perfectly reconstructed. In Fig. 5(b), a transmission error occurred at the edge location and the edge information in the prediction error signal has been halved, so that the edge disappeared in the reconstructed signal; the original signal cannot be reconstructed. This fact will limit the use of 1-D PM-DPCM. In the next subsection, we shall show that such a problem does not occur in 2-D PM-DPCM.

2.2 Two-Dimensional PM-DPCM

2-D PM-DPCM employs 2-D median predictors. We shall consider two types of 2-D median predictors which are defined as follows:

$$\begin{aligned} \text{Med1: } \hat{y}(m,n) &= \text{median}\{y(m-1,n+1), y(m-1,n), y(m,n-1)\} \quad (7) \\ \text{Med2: } \hat{y}(m,n) &= \text{median}\{y(m-1,n-1), y(m-1,n), \\ &\quad y(m-1,n+1), y(m,n-1)\} \end{aligned} \quad (8)$$

The predictors in (7) and (8) will be referred to as Med1 and Med2 predictors, respectively. In (8), the median of four values is the average of the two median values. As with the 1-D case,

the 2-D PM-DPCM has the error isolation property: Observations 1 and 2 can be extended directly to the 2-D case. Fig. 6 shows the behavior of 2-D PM-DPCM around edge locations. The original vertical edge is reconstructed under noise-free conditions. When a transmission error occurs at an edge location, the 2-D PM-DPCM systems distorts the edge but retains most edge information. It should be noted that the PM-DPCM with Med2 performs considerably better than the one with Med1. Similar observations can be made for edges with other directions.

3. STATISTICAL PROPERTIES OF THE PM-DPCM

In this section, the variance of the prediction errors associated with the 1-D PM-DPCM are derived and compared with those of the standard DPCM. Again, the quantization effects are neglected throughout this section. The prediction error $x(n)$ in the PM-DPCM is

$$\begin{aligned} x(n) &= y(n) - \text{median}\{y(n-i), i=1, \dots, M\} \\ &= \text{median}\{y(n) - y(n-i), i=1, \dots, M\}. \end{aligned} \quad (9)$$

The variance of $x(n)$ can be calculated if the joint probability density function (pdf) for $y(n) - y(n-i)$, $i=1, \dots, M$ in (9) is known. Assumed that the input signal $y(n)$ is an AR (autoregressive) process with a Gaussian distribution. Specifically,

$$y(n) = 0.9y(n-1) + w(n), \quad (10)$$

where $w(n)$ is an independent identically distributed (i.i.d.) white Gaussian noise of $N(0,1)$. Then we have $\text{Var}[x(n)] = E[x^2(n)]$ because $y(n)$ is a WSS process with a Gaussian distribution and accordingly $E[x(n)] = E[\text{median}\{y(n) - y(n-i), i=1, \dots, M\}] = 0$.

Therefore, $E[y(n-i)] = E[y(n)] = 0$. Therefore,

$$\begin{aligned} \text{Var}[x(n)] &= \\ &= \int_{R^M} [\text{median}\{v_1, \dots, v_M\}]^2 p(v_1, \dots, v_M) dv_1 \dots dv_M \end{aligned} \quad (11)$$

where $v_i = y(n) - y(n-i)$, $i=1, \dots, M$ and $p(v_1, v_2, \dots, v_M)$ is the joint pdf of v_1, v_2, \dots, v_M . $\text{Var}[x(n)]$ is evaluated numerically for $M=3$, and we get $\text{Var}[x(n)] = 1.711$. The variance of the prediction errors of the optimal linear predictor for the AR process in (10) is equal to the variance of $w(n)$ which is one. As expected, the median predictor has a larger variance than the optimal linear predictor. This fact is also true for 2-D median predictors. Discussions on the extension to the 2-D case is straightforward but somewhat cumbersome, so omitted here.

4. EXPERIMENTAL RESULTS

The PM-DPCM and other DPCM systems are applied to real image signals to compare their performance characteristics. The predictors considered include Med1 and Med2 for 2-D PM-DPCM, the 1-D median predictor of span 3, the 1-D linear predictor $\hat{y}(m,n) = 0.9y(m,n-1)$, some 2-D linear predictors and the FIR-median hybrid (FMH) predictor [4]. The FMH and 2-D linear predictors are defined as follows:

$$\begin{aligned} \text{FMH: } \hat{y}(m,n) &= \text{median}\{y(m-1,n), y(m,n-1), y(m-1,n), \\ &\quad [p] \text{ where} \\ &\quad f = 0.5y(m,n-1) + 0.25[y(m-1,n) + y(m-1,n+1)], \\ &\quad p = y(m,n-1) + y(m-1,n) - y(m-1,n-1)\} \end{aligned} \quad (12)$$

$$\text{Lin1: } \hat{y}(m,n) = 0.9y(m-1,n) + 0.9y(m,n-1) - 0.81y(m-1,n-1) \quad (13)$$

$$\text{Lin2} : \hat{y}(m,n) = 0.25y(m-1,n) + 0.5y(m,n-1) + 0.25y(m-1,n+1) \quad (14)$$

The Lin1 predictor in (13) is an optimal linear predictor for a 2-D AR process, and the Lin2 predictor in (14) has been proposed for encoding television signals[5]. Lena image has 256x256 pixels. All DPCM systems considered in this section employ the 4-bit quantizer specified in Table 2. It is assumed that transmission bit errors occur with the same probability, say P_e , at each bit of $x(n)$.

Fig. 7(a) shows the original image which consists of 256x256 pixels with 8-bits of resolution. Under noise-free conditions ($P_e = 0$), all the DPCM systems produced images which are very close to the original; the reconstructed images will not be presented. Fig. 7 (b)-(h) show the reconstructed DPCM images when the transmission bit error probability $P_e = 0.005$. It is seen that the 2-D PM-DPCM systems outperformed the rest. Between the two 2-D PM-DPCM systems, the one employing the Med2 predictor performed better than the other; The 2-D PM-DPCM with Med1 distorted some edges. The DPCM with Lin2 is seen to be more robust to transmission errors than the DPCM with Lin1. It is apparent that the DPCM systems with Lin1, FMH and the 2-D linear predictor are vulnerable to transmission errors. In 1-D PM-DPCM some edges are lost due to transmission errors at edge locations.

5. CONCLUSIONS

A DPCM system using a median-type predictor has been proposed and its performance characteristics were analyzed. It was shown that the system is insensitive to transmission errors. The experimental results indicate that the PM-DPCM can outperform the conventional DPCM when transmission errors occur, and that the former performs like the latter under noise-free conditions. In addition, the implementation of median predictors is very simple. The PM-DPCM is a useful alternative to conventional DPCM systems in encoding images.

6. REFERENCES

- [1] N.S. Jayant and P. Null, *Digital Coding of Waveforms: Principles and Application to Speech and Video*, Prentice Hall, 1984.
- [2] M. C. W. van Buul, "Hybrid DPCM, a combination of PCM and DPCM," *IEEE Trans. Commun.*, vol. COM-26, pp.362-368, Mar. 1978.
- [3] K. N. Ngan and R. Steele, "Enhancement of PCM and DPCM images corrupted by transmission error," *IEEE Trans. Commun.*, vol. COM-30, pp.257-265, Jan. 1982.
- [4] J. Salo, Y. Neuvo and V. Haneenaho, "Improving TV picture quality with linear-median type operators," *IEEE Trans. Consum. Electron.*, vol. CE-34, pp.373-379, Aug. 1988.
- [5] P. Pirsch, "A new predictor design for DPCM coding of TV signals," *Conf. Rec. ICC'80*, pp.31.2.1-31.2.5, Jun. 1980.

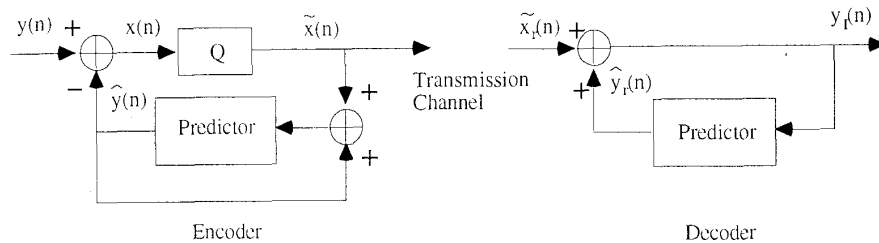


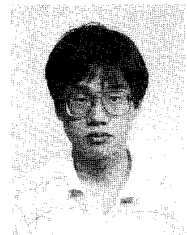
Figure 1. The DPCM System

BIOGRAPHIES



Dong Hee Kang received the B.S. degree in electronics engineering in 1986 from Hanyang University, Seoul, Korea, and the M.S. degree in electrical engineering from Korea Advanced Institute of Science and Technology (KAIST), Seoul, Korea, in 1988. He is currently working towards the Ph. D. degree in electrical engineering at KAIST, Taejon, Korea.

From 1988 to 1991, he was a member of data communication laboratory of DACOM, Seoul, Korea, working on data communication. His main research interests are signal processing, nonlinear filtering, pattern recognition, and communication.



Jin Ho Choi was born in Seoul, Korea, in 1967. He received the B.S. degree in electronics engineering from Sogang University, Seoul, Korea, in 1989 and the M.S. degree in electrical engineering from Korea Advanced Institute of Science and Technology (KAIST), Seoul, Korea, in 1991. He is currently working towards the Ph. D. degree in electrical engineering at KAIST. His research interests are in

signal and system estimation theory, nonlinear filtering theory, and array signal processing.



Yong Hoon Lee received the B.S. and M.S. degree in electrical engineering from Seoul National University, Seoul, Korea, in 1978 and 1980, respectively, and the Ph. D. degree in systems engineering from the University of Pennsylvania, Philadelphia, in 1984.

From 1984 to 1988, he was an assistant professor at the Department of Electrical and Computer Engineering, State University of New York at Buffalo.

Since 1989 he has been with KAIST, where he is currently an Associate Professor. His research activities are in the areas of one- and two-dimensional signal processing.

Choon Lee, for biography and photo see the paper "A New Two-Layered Video Compression Scheme for Multiple Applications" by Choon Lee, D-H. Lee, J-S. Park, Y-G. Kim

Table 1. The quantizer specifications. For a negative input value x , the representative value y is determined with its absolute value $|x|$ and $-y$ is given to the output

x	y
$0 \leq x \leq 4$	2
$4 \leq x \leq 9$	6
$9 \leq x \leq 15$	11
$15 \leq x \leq 21$	18
$21 \leq x \leq 30$	25
$30 \leq x \leq 41$	34
$41 \leq x \leq 59$	48
$59 \leq x \leq 255$	70

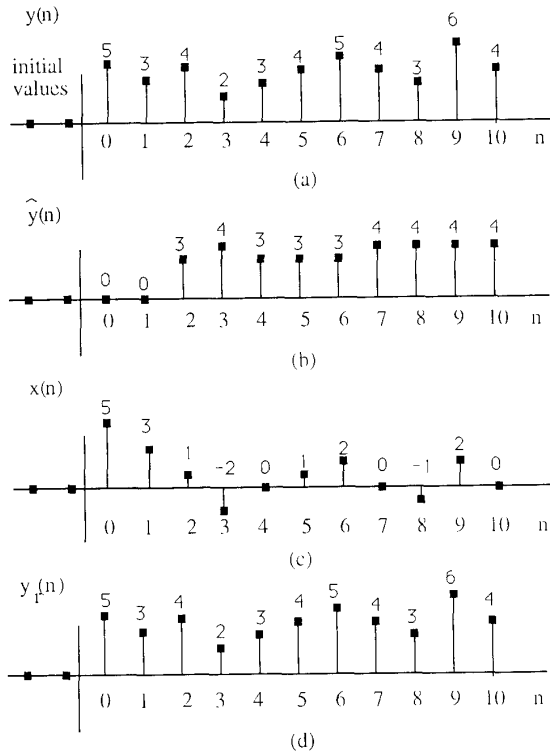


Figure 2. (a) The original signal, (b) outputs of the median predictor of span 3, (c) outputs of the encoder, (d) the reconstructed signal (Quantization effect is ignored.)

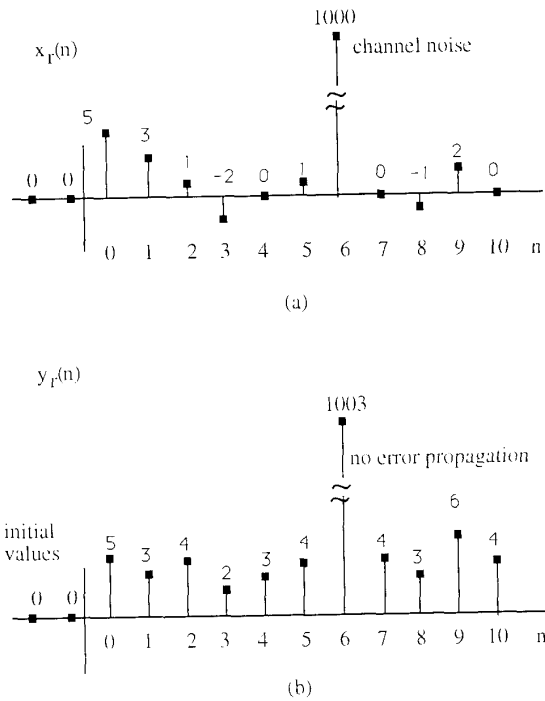


Figure 3. (a) $x(n)$ corrupted by channel noise, (b) the reconstructed signal from corrupted $x(n)$

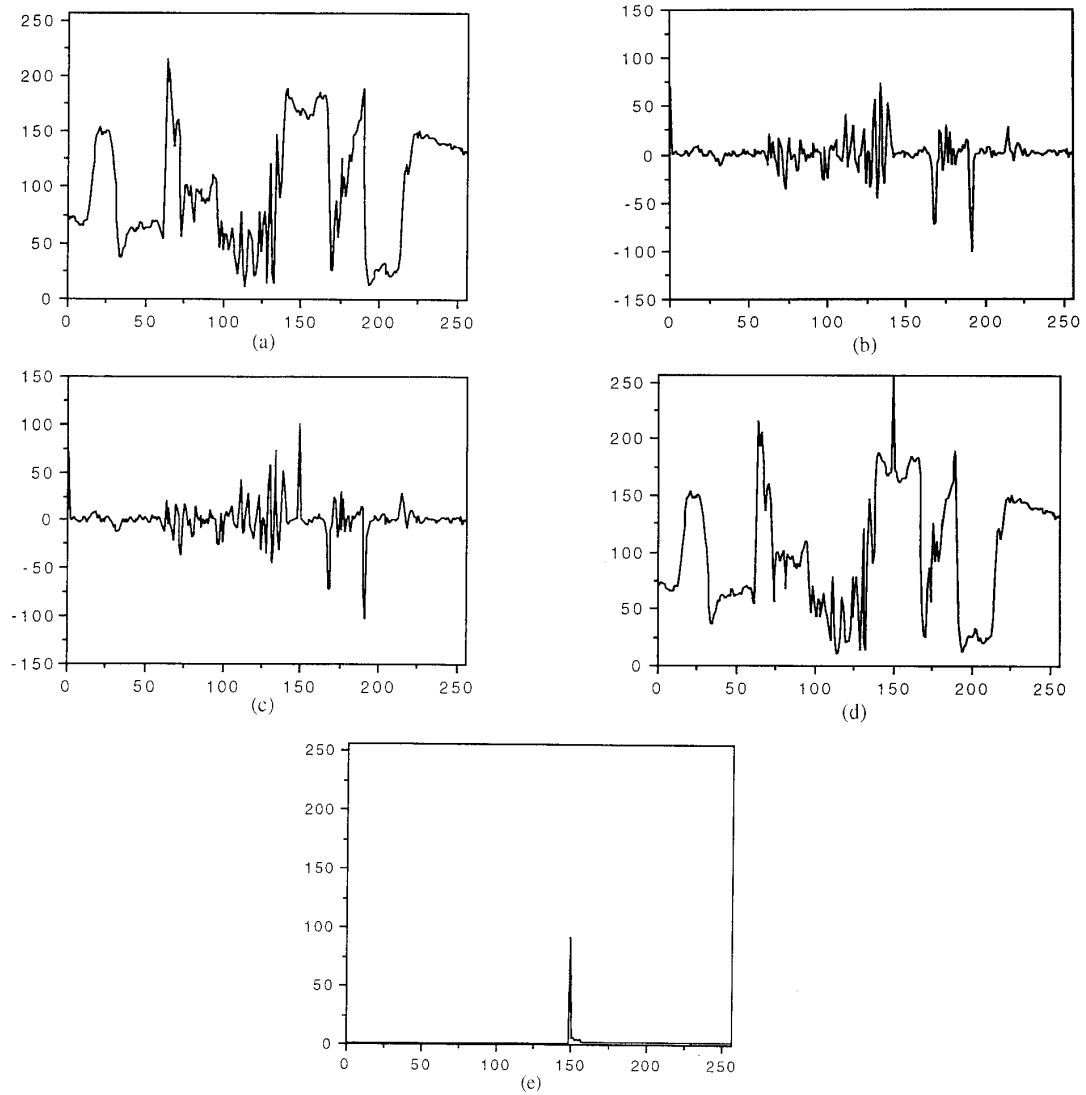


Fig. 4. An example for one row of real image signals. (a) the original signal $y(n)$, (b) the prediction error signal $x(n)$, (c) the received error signal $x_r(n)$, (d) the reconstructed signal $y_r(n)$, (e) the difference between $y(n)$ and $y_r(n)$, $|y(n) - y_r(n)|$.

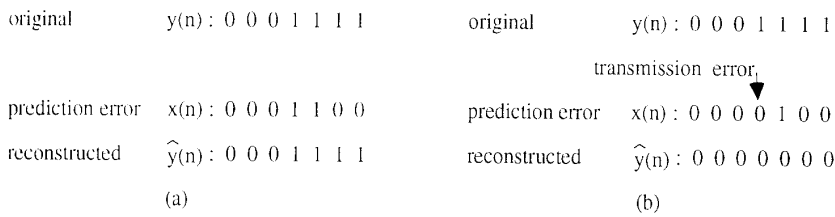


Fig. 5. The 1-D PM-DPCM of a binary input signal with an edge. All initial values are zero and $M=3$. (a) Noise-free case, (b) Noisy case.

original	0 0 0 0 0 0 0						
	0 0 0 1 1 1 1						
	0 0 0 1 1 1 1						
	0 0 0 1 1 1 1						
	0 0 0 1 1 1 1						
prediction	0 0 0 0 0 0 0						
error	0 0 0 1 1 1 1						
	0 0 0 0 0 0 0						
	0 0 0 0 0 0 0						
	0 0 0 0 0 0 0						
	0 0 0 0 0 0 0						
received	0 0 0 0 0 0 0	transmission	received	0 0 0 0 0 0 0			
prediction	0 0 0 1 1 1 1	error	prediction	0 0 0 1 1 1 1			
error	0 0 0 1 0 0 0		error	0 0 0 1 0 0 0			
	0 0 0 0 0 0 0			0 0 0 1/2 0 0 0			
	0 0 0 0 0 0 0			0 0 0 1/2 0 0 0			
	0 0 0 0 0 0 0			0 0 0 1/2 0 0 0			
reconstructed	0 0 0 0 0 0 0		reconstructed	0 0 0 0 0 0 0			
by PM-DPCM	0 0 0 1 1 1 1		by PM-DPCM	0 0 0 1 1 1 1			
with Med1	0 0 0 2 1 1 1		with Med2	0 0 0 3/2 1 1 1			
	0 0 0 1 1 1 1			0 0 0 1 1 1 1			
	0 0 0 1 1 1 1			0 0 0 1 1 1 1			

Fig. 6. The 2-D PM-DPCM of a 2-D binary input signal with a vertical edge.

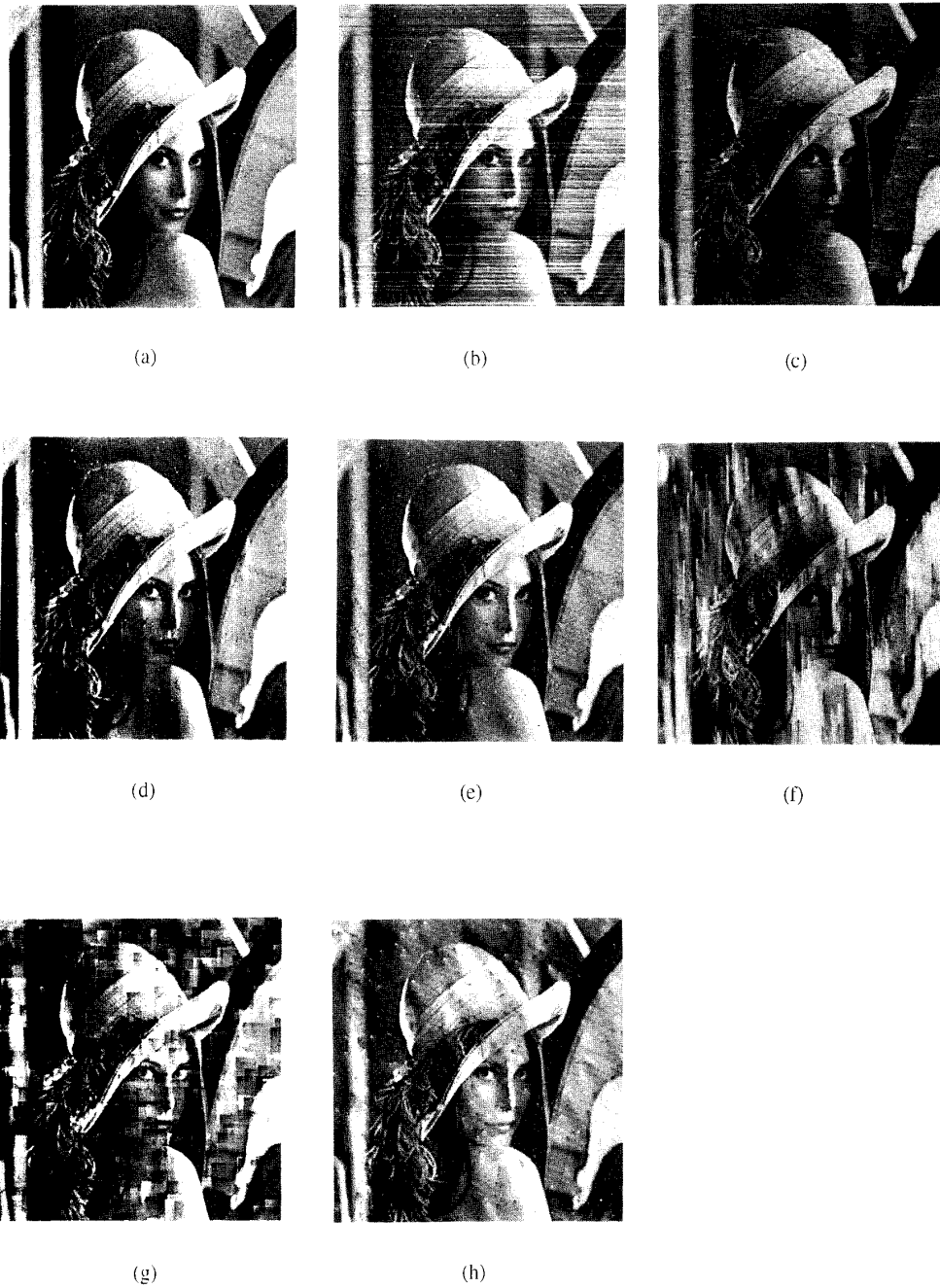


Fig. 7. (a) Lena image. When $P_e = 0.005$, experimental results from (b) the 1-D median predictor, (c) the 1-D linear predictor, (d) the Med1 predictor, (e) the Med2 predictor, (f) the FMH predictor, (g) the Lin1 predictor, (h) the Lin2 predictor.